(Preprint) AAS XX-XXX

COMPARISON OF THE IMPACT OF A LEO AND A MEO CONSTELLATION ON SELECTED OBSERVATORIES

Benjamin Salak*

The purpose of this paper is to examine how satellite constellations in medium Earth orbit (MEO) and low Earth orbit (LEO) impact observatories. The approach used to study the impact on these constellations is to simulate the motion of the constellations and determine how often they are above a set of selected observatories. The resulting impact is quantified by how many times satellites are present within different fields of view. An individual LEO or MEO constellation does not have a significant impact on usable observatory hours, with time lost ranging from 1 minute to 5 hours over an 84-hour period of darkness. The introduction of multiple LEO and MEO constellations would further decrease the usable observatory hours.

INTRODUCTION

Satellite constellations are becoming more and more common. In 2022, there were approximately 5,500 satellites in orbit, with some projections estimating that by 2030 there will be over 58,000.[1] The main driver of this expansion are low Earth orbit satellite (LEO) constellations.[1] LEO orbits are from 300 km to 2,000 km above the Earth's surface. The other two major orbital categories are medium Earth orbits (MEO) from 2,000 km to 35,000 km and geosynchronous orbits (GEO), which are located at 35,686 km above the Earth's surface.[2] LEO constellations offer numerous benefits. Since LEO satellites are lower, communications are quicker, and images have a greater resolution than those with the same equipment from MEO and GEO satellites. However, LEO constellations do have drawbacks. LEO satellites can only view one location on Earth for approximately 10 minutes before moving out of range, meaning that for continuous communication, more satellites are needed in LEO than in MEO constellations.[2] The need for more satellites increases maintenance costs.[2] The impact of all these satellite clusters is being felt in the astronomy community. Figure 1 is an image from the CTIO/NOIRLab/NSF/AURA/DECam DELVE Survey. The impact of the satellite trails is clearly visible.

* Graduate Student, Aerospace and Engineering Mechanics, The University of Alabama, Tuscaloosa, Alabama, 35487.

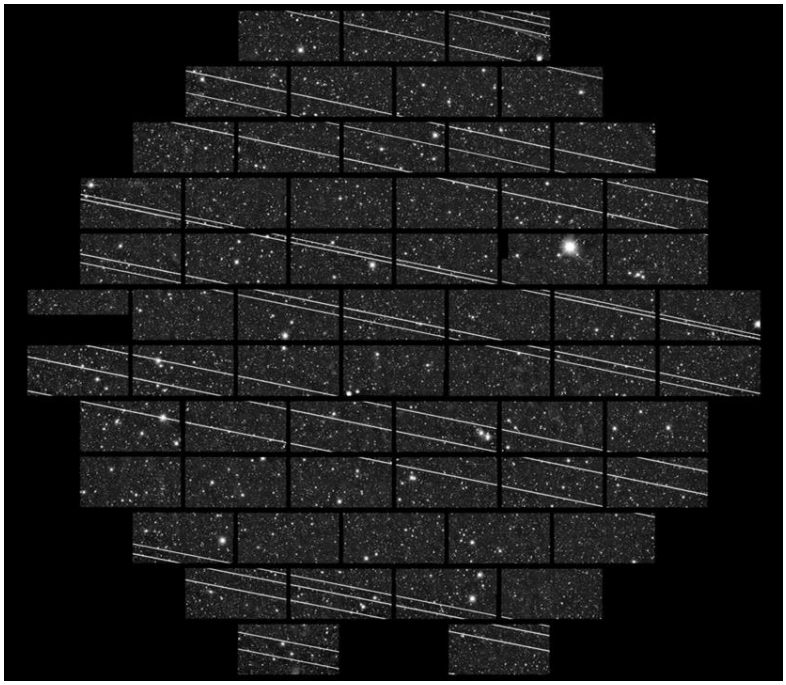

Figure 1. Deep Field Image with Satellite Trails.

Recently a satellite from Applied Satellite Technology named Blue Walker 3 was launched into orbit. This new communications satellite has reached a peak magnitude of 0.4.[*] This magnitude is comparable to some of the brightest stars visible to the naked eye from Earth. The Blue Walker 3 is stationed in LEO; however, MEO is another orbit category that is considered a "goldilocks zone" and poised for increased use as it has lower latency than GEO orbits and better Earth coverage per satellite than LEO orbits.[†] Both LEO and MEO constellations are analyzed in this paper.

LITERATURE REVIEW

The purpose of this literature review is to discuss the published knowledge focused on examining the impact of satellite constellations on observatories. "Impact of Satellite Constellations on Astronomical Observations with ESO Telescopes in the Visible and Infrared Domains" by Oliver R. Hainaut and Andrew P. Williams provides a focused analysis on this topic. The major difference in the analysis conducted for this paper and the one described in the Hainaut and Williams paper is that this is a simulation-based analysis, while their analysis used statistical distributions. Hainaut and Williams provide the following conclusion, which they characterize as conservative: wide field images from visual Earth-based telescopes will be severely affected.[3] They also note that detailed simulation using actual satellite orbits will be needed to refine their estimates.[3] This current paper provides a detailed simulation for certain orbital constellation conditions.

[*] www.space.com/bluewalker-3-prototype-satellite-brightest-objects-sky

[†] www.kratosdefense.com/constellations/articles/is-meo-poised-for-new-growth-as-satellite-market-shifts

The second paper that discusses the impact of satellite constellations on observatories is "Impact of Satellite Constellations on Optical Astronomy and Recommendations toward Mitigations," by Connie Walker.[4] The conclusions of this paper focus on satellite altitude and how it affects observatories. LEO satellites under 600 km have the least impact on observatories as the intersections occur during the twilight hours; however, satellites above 600 km are illuminated during the night (not only at twilight) and therefore have a greater impact. Each altitude range primarily impacts observatories located at the middle latitudes.[4] Walker's paper leverages data provided by Oliver Hainaut, who co-authored the first paper described above. The goal of this current paper is to produce results using simulated constellations for multiple observatories in different latitudes.

METHODS

Low Earth Orbit (LEO)

The LEO constellation used in this paper is a hypothetical constellation that provides 90% to 95% Earth coverage but has no real-world twin. This coverage is based on a 90% to 95% Earth coverage model from the Congressional Budget Office (CBO) large constellation report.[2] Figure 2 shows pictures of the LEO constellation taken from this report.

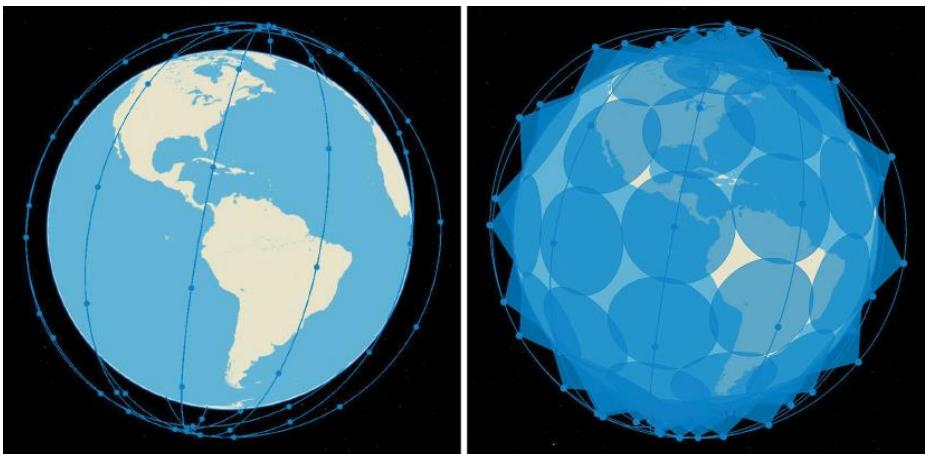

Figure 2. LEO Constellation Layout.

This constellation relies on orbits with altitudes of 1,000 km. The constellation includes 72 satellites. There are six evenly spaced orbit planes at 80 degrees of inclination with 12 evenly spaced satellites in each orbit plane.

Middle Earth Orbit (MEO)

The MEO constellation is a hypothetical constellation that provides coverage comparable to that of the LEO and also has no real-world twin. This coverage is also based on a 90% to 95% Earth coverage model from the CBO large constellation report.[2] Figure 3 shows a picture of the MEO constellation.

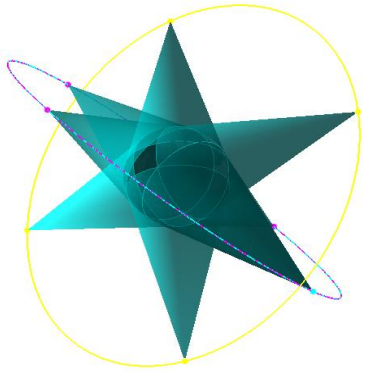

Figure 3. MEO Constellation Layout.

This constellation relies on orbits with altitudes of 18,000 km. The constellation includes eight satellites. There are two orbit planes at 45 degrees of inclination with four evenly spaced satellites in each orbit plane.

Observatory Selection

A subset of the observatories with the largest telescopes on Earth was compiled and is shown in Table 1. The five locations are spread out across latitudes and longitudes to ensure potential effects of the satellite constellations can be documented on different continents.

Table 1. Observatory Data.

Observatory	Location	Telescope Size (m)	Latitude (deg)	Longitude (deg)	Time Zone UTC
1. Extremely Large Telescope (ELT)	Cerro Armazones, Chile	39	-24.5894	-70.1919	-3
2. Thirty Meter Telescope (TMT)	Mauna Kea, Hawaii	30	19.8327	-155.4816	-10
3. Gran Telescopio Canarias (GTC)	La Palma, Spain	10.4	28.7561	-17.8917	0
4. Hobby-Eberly	Fort Davis, Texas	10	30.6814	-104.0147	-6
5. South African Large Telescope (SALT)	Karoo, South Africa	9.8	-32.3759	20.8108	2

These observatories are important as they are all large visual observatories. The wide field visual astronomy telescopes are the observatories the most at risk from satellite intersections. Enormous investments have been made in these large installations, and some were built in isolated, high altitude, desert-like areas to escape clouds and light pollution.

Method of Simulation

A MATLAB based simulation is used to simulate the satellite positions. The simulation relies on elliptic *f* and *g* functions to calculate a new location for the satellite after a delta time. This new location is evaluated to see if it intersects with the observatory. The new location is also evaluated to determine if the satellite is illuminated by the sun. The simulation time is evaluated to determine if it is nighttime at the observatory that the satellite is intersecting. This analysis process will repeat for the entire simulation time.

Since the constellations are provided by the CBO report, the orbital elements can be defined for each satellite, and the satellite's initial position can be defined. The simulation uses input parameters a, e, i, θ_0^*, ω, and Ω. The a value is the semi-major axis, which is the radius of the orbit, since all the orbits in this analysis are circular. The e value is the eccentricity, which is 0 since the orbits are all circular. The i value represents inclination and varies depending on which orbit is being analyzed. The θ_0^* value represents the true anomaly, which varies depending on the satellite in each orbit. The initial θ_0^* values are all known quantities. The ω represents the argument of periapsis. The Ω represents the right ascension of the ascending node (RAAN). The θ value represents the argument of true anomaly, which is the sum of ω and θ_0^*.

From the orbital element values, the radius vector, $\bar{r}_{\text{perifocal}}$, can be calculated. This vector is the 3D position of the satellite relative to the focus of the orbit, in this case Earth. The easiest way to express this vector is in the perifocal frame.

The perifocal frame is defined with the e vector pointing toward the periapsis, the p vector pointing in the orbital plane in the direction of a true anomaly angle of 90 degrees, and the q vector pointing out of the orbital plane in the direction of the angular momentum vector. Equation (2) is the formula for the perifocal frame.

Where h is the specific angular momentum defined in Equation (1).

$$h = \sqrt{\mu_{\text{Earth}} \cdot \text{a} \cdot (1 + e)} \tag{1}$$

$$\bar{r}_{\text{perifocal}} = \frac{h^2}{\mu_{\text{Earth}}} \cdot \frac{1}{1 + e \cdot \cos(\theta_0^*)} \cdot \begin{bmatrix} \cos(\theta_0^*) \\ \sin(\theta_0^*) \\ 0 \end{bmatrix} \tag{2}$$

Next the velocity vector, $\bar{v}_{\text{perifocal}}$, can be calculated from the same orbital elements. The result, also in the perifocal frame, is expressed below with Equation (3):

$$\bar{v}_{\text{perifocal}} = \frac{\mu_{\text{Earth}}}{h} \cdot \begin{bmatrix} -\sin(\theta_0^*) \\ e + \cos(\theta_0^*) \\ 0 \end{bmatrix} \tag{3}$$

With the r and v values represented as vectors in the perifocal frame, a transformation is used to represent the vectors in an XYZ frame. This is done to move to a universal coordinate system instead of the orbit-specific perifocal systems. The perifocal coordinate system is orbit specific as the p and q quantities are relative to the orbital plane of each orbit. The XYZ frame is centered at Earth so all satellite positions can be compared. The direction cosine matrix (DCM) to move between these frames is given in Equation (4), where *c* is cosine and *s* is sine.

$$DCM = \begin{bmatrix} c_\Omega c_\theta - s_\Omega c_i s_\theta & -c_\Omega s_\theta - s_\Omega c_i c_\theta & s_\Omega s_i \\ s_\Omega c_\theta + c_\Omega c_i s_\theta & c_\Omega c_i c_\theta - s_\Omega s_\theta & -c_\Omega s_i \\ s_i s_\theta & c_\theta s_i & c_i \end{bmatrix} \tag{4}$$

By using the DCM from Equation (4), the $\bar{r}_{\text{perifocal}}$ and $\bar{v}_{\text{perifocal}}$ vectors defined in the perifocal frame from Equations (2) and (3) can be transformed into this Earth-centered XYZ frame. The $\bar{r}_{\text{XYZ}}$ and $\bar{v}_{\text{XYZ}}$ vector transformations are Equations (5) and (6), respectively.

$$\bar{r}_{\text{XYZ}} = DCM \cdot \bar{r}_{\text{perifocal}} \tag{5}$$

$$\bar{v}_{\text{XYZ}} = DCM \cdot \bar{v}_{\text{perifocal}} \tag{6}$$

With the position and velocity of the satellite established at its initial position, the relationship between this position and the initial time, defined from the time since periapsis, must also be established. The variable t_o represents this initial time and can be computed.

This value is dependent on the eccentric anomaly, *E*, which is defined in Equation (7).

$$E = 2 \cdot \text{atan}\left(\frac{\theta_0^*}{2}\right) \cdot \sqrt{\frac{1-e}{1+e}} \tag{7}$$

The mean anomaly, *M*, can then be calculated, as shown in Equation (8).

$$M = E - e \cdot \sin(E) \tag{8}$$

The orbital period, *P*, which is computed in Equation (9), is also needed to find the time since periapsis.

$$P = \frac{2 \cdot \pi}{\mu_{\text{Earth}}} \cdot a^{\frac{3}{2}} \tag{9}$$

The results from Equations (8) and (9) are used to compute the time since periapsis, t_o, with Equation 10.

$$t_o = M \cdot \frac{P}{2 \cdot \pi} \tag{10}$$

To use the *f* and *g* relationships in the elliptical format, the final time is also needed.

The initial time, t_o, is the configuration at the start of the simulation. The final time, t_f is some delta time, Δt, away from the initial position, θ_0^*. The delta time can vary to increase and decrease the resolution of the simulation. The final time is computed in Equation (11).

Once this value is calculated, the θ_f^* value can be calculated and used in the *f* and *g* relationships.

$$t_f = t_o + \Delta t \tag{11}$$

Next, the new mean anomaly can be calculated with Equation (12).

$$M_f = \frac{2 \cdot \pi \cdot t_f}{P} \tag{12}$$

The new eccentric anomaly can be calculated with Equation (13).

$$E_f - e \cdot \sin(E_f) = M_f \tag{13}$$

This equation requires an iterative Newtonian solver to compute. An example of an interactive solver that can compute this quantity can be found under algorithm 3.1 in *Orbital Mechanics for Engineering Students*.[5]

The θ_f^* value can be calculated with Equation (14).

$$\theta_f^* = 2 \cdot \text{atan}\left(\tan\left(\frac{E_f}{2}\right)\right) \cdot \sqrt{\frac{1+e}{1-e}} \tag{14}$$

All the variables are calculated that are necessary to compute the *f* and *g* values. The formulas for the *f* and *g* functions are Equations (15) and (16), respectively.

$$f = 1 - \frac{r}{p}\left[1 - \cos\left(\theta_f^* - \theta_0^*\right)\right] \tag{15}$$

$$g = \frac{rr_0}{\sqrt{\mu p}} \sin(\theta_f^* - \theta_0^*)\overline{v_o} \tag{16}$$

The *f* and *g* functions can be combined, as shown in Equation (17). This equation represents the r vector, $\bar{r}_{\text{XYZ f}}$, at the new position, θ_f^*, which is after a delta time has elapsed.

$$\bar{r}_{\text{XYZ f}} = f \cdot \bar{r}_{\text{XYZ}} + g \cdot \bar{v}_{\text{XYZ}} \tag{17}$$

The XYZ vector is currently in an Earth-centered reference frame, but this frame does not account for the rotation of the Earth as the X axis always points at the vernal equinox.

An Earth-centered, Earth-fixed XYZ coordinate frame is needed. This frame requires the angle that the Earth has rotated through during the delta time between the θ^* values. This angle is defined in Equation (18).

$$\theta = \omega_E(t - t_0) \tag{18}$$

This θ value can be used in a new DCM to convert between the two XYZ frames, represented in Equation (19). This frame is necessary to plot the position of the satellite on a ground track as both the satellite and Earth's surface have moved.

$$\text{DCM} = \begin{bmatrix} \cos(\theta) & \sin(\theta) & 0 \\ -\sin(\theta) & \cos(\theta) & 0 \\ 0 & 0 & 1 \end{bmatrix} \tag{19}$$

The transformation equation to move between the two frames is shown in Equation (20), using the DCM from Equation (19).

$$\bar{r}_{\text{XYZ f rot}} = \text{DCM} \cdot \bar{r}_{\text{XYZ f}} \tag{20}$$

An algorithm can be used to compute the right ascension and declination of the satellite, given the orbital elements and the current satellite position from Equation 20. This algorithm is an excerpt from algorithm 4.6 in *Orbital Mechanics for Engineering Students*.[5]

Compute the magnitude of $\bar{r}_{\text{XYZ f rot}}$ using Equation (21).

$$|\bar{r}_{\text{XYZ f rot}}| = \sqrt{{r_{X\,f\,rot}}^2 + {r_{Y\,f\,rot}}^2 + {r_{Z\,f\,rot}}^2} \tag{21}$$

Compute the DCM of $\bar{r}_{\mathrm{XYZ\,f\,rot}}$. In this case, the DCM is represented by individual equations, Equations (22) through (24), that will be used by later equations.

$$l = \frac{r_{X\,f\,rot}}{|\bar{r}_{\mathrm{XYZ\,f\,rot}}|} \tag{22}$$

$$m = \frac{r_{Y\,f\,rot}}{|\bar{r}_{\mathrm{XYZ\,f\,rot}}|} \tag{23}$$

$$n = \frac{r_{Z\,f\,rot}}{|\bar{r}_{\mathrm{XYZ\,f\,rot}}|} \tag{24}$$

Calculate the declination, δ, with Equation (25).

$$\delta = \sin^{-1}(n) \tag{25}$$

Calculate the right ascension, α, with Equation (26).

$$\alpha = \begin{cases} \cos^{-1}\left(\frac{l}{\cos(\delta)}\right), & (m > 0) \\ 360 - \cos^{-1}\left(\frac{l}{\cos(\delta)}\right), & (m < 0) \end{cases} \tag{26}$$

The α and δ values can then be plotted on a Mercator projection of the Earth. The α value is the angle measured from the vernal equinox along the equator. The δ value is the angular position of the object north or south of the equator.

The observatory positions must also be written in a format that can be compared with the α, δ, and XYZ values so equations can be written to establish when a satellite intersects with an observatory.

The observatories have latitude and longitude values, which are analogous to α and δ values. These latitude and longitude values can be transformed into XYZ coordinates by using the following matrix.

$$\overline{\text{observatory}}_{\mathrm{XYZ}} = \begin{bmatrix} r_{\mathrm{Earth}} \cdot \cos(\mathrm{lat}) \cdot \cos(\mathrm{lon}) \\ r_{\mathrm{Earth}} \cdot \cos(\mathrm{lat}) \cdot \sin(\mathrm{lon}) \\ r_{\mathrm{Earth}} \cdot \sin(\mathrm{lat}) \end{bmatrix} \tag{27}$$

With the results from Equation (27), all the values required to compare the observatory position to the satellite position at any given time are known.

This comparison is computed with a dot product angle. The angle represents the angular separation of the two vectors. If the angle is 0, the satellite is directly above the observatory. This angle can be checked against determined field of view (FOV) angles to see if it impacts an observatory under different observing conditions. The dot product angle is calculated with Equation (28).

$$\theta = \text{acos}\left(\frac{\bar{r}_{\text{XYZ f rot}} \cdot \overline{\text{observatory}}_{\text{XYZ}}}{\left|\overline{\text{observatory}}_{\text{XYZ}}\right| \cdot \left|\bar{r}_{\text{XYZ f rot}}\right|}\right) \tag{28}$$

This angle is evaluated at 1 degree, 5 degrees, and 10 degrees. The smallest grouping the angle fits into is where it is counted. The impact to an observatory is quantified by looking at the percentage of points that intersect with the observatory during nighttime.

The final portion of the analysis involves reducing the amount of satellite observatory intersection data. This process includes determining which intersections occur during the day at each observatory because observing times can only be interrupted at visual telescopes when it is dark.

The second reduction is determining if the satellite is reflecting the light of the sun. A satellite can only impact an observatory if it is dark and the satellite is reflecting sunlight. The reflected sunlight is what is picked up by the telescope and can be seen as satellite trails (see Figure 1).

Carrying out the first reduction requires using the Julian Date (JD). The satellite constellations are conceptual, so their initial positions can be defined arbitrarily. The start date is chosen as December 1, 2023, at 6:00 pm UTC. Equation (29) converts this date to a JD. The time variables are *y* for years, *m* for months, and *d* for days. Where t_{UTC} is the UTC time formatted in decimal hours.

$$J_0 = 367 \cdot y - \text{INT}\left\{\frac{7 \cdot (y + \text{INT}\left(\frac{m+9}{12}\right))}{4}\right\} + \text{INT}\left(\frac{275 \cdot m}{9}\right) + \text{d} + 1721013.5 + \frac{t_{\text{UTC}}}{24} \tag{29}$$

The decimals of a JD output represent hours in a day. If the decimal is between 0.25 and 0.75, then it is dark out in UTC time. By using the information in Table 1, the decimals can be offset based on UTC plus or minus hour values. With this time zone offset, the local day and night can be established.

To detect if the Earth is in shadow, the process outlined by Pedro Escobal in the 1976 text *Methods of Orbit Determination* is used.[6]

This process assumes that the sun generates a cylinder, which is the diameter of Earth, that represents the shadow cast by the sun. Vector math is used to determine if the current satellite position is inside this cylinder. There are two conditions that need to be satisfied for the satellite to be considered in shadow. The first is the angle ψ. This angle is the angle between the sun vector and the Earth vector. The origin for both vectors is the center of the Earth. The sun vector is assumed to be in the direction [1 0 0]. The distance of the sun vector is the distance from the Earth to the sun. The satellite vector in XYZ is already known. Equation (30) shows the calculation of the angle ψ.

$$\cos(\psi) = \frac{\overline{\text{sunXYZ}} \cdot \bar{r}_{\text{XYZ f}}}{\left|\overline{\text{sunXYZ}}\right| \cdot \left|\bar{r}_{\text{XYZ f}}\right|} \tag{30}$$

When the cosine of ψ is less than 0, the first condition is met.

The second condition is that the a value is less than the radius of the Earth. The a value is equal to Equation (31). (Note: This a value does not represent the semi-major axis.)

$$a = |\bar{r}_{\mathrm{XYZ\,f}}| \cdot \sin(\psi) \tag{31}$$

When both the a value and the $\cos(\psi)$ conditions are met, the satellite is in shadow.

Assumptions and Limitations of the Method of Simulation

There are assumptions in the model presented in this paper:

- The Earth is assumed to be a perfect circle so that latitude and longitude conversions can easily be made for each of the observatories.
- The altitude of the observatories is ignored although some of the chosen observatories are in mountainous terrain.
- The Earth is assumed to be a point mass, an assumption that neglects any effects of the Earth's oblateness.
- To compute the time in shadow, the assumption that the Earth and sun both lie on the ecliptic plane is made.
- To compute day and night, complete darkness from 6:00 pm to 6:00 am local time is assumed. This means that all 24-hour days are considered to have 12 hours of absolute daylight and 12 hours of absolute darkness.

There are limitations to the model presented in this paper:

- The smaller the delta time of the simulation, the more likely the simulation is to detect an intersection, but this small delta time causes the simulation to run significantly slower for longer data sets.
- The reflectivity of the satellite is not considered. No matter the distance between the satellite and observatory and their relative positions, if the conditions for an intersection are met, then the observatory can see the satellite.

RESULTS

The specific configuration used to generate the result data is outlined here. The conditions for simulating the LEO and MEO satellites were the same. The simulation time was 7 days with a delta time step of 5 sec. For the FOV grading, half angles of 0.5, 2.5, and 5 degrees were used.

LEO Results

Figure 4 shows the set of satellite orbits from an Earth-fixed nonrotating frame. This plot is a check to ensure that the orbits are correctly matching what the CBO theoretical constellation specified.

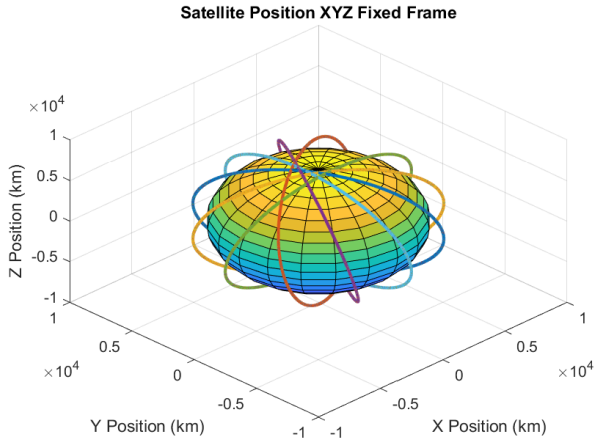

Figure 4. LEO Orbit Track Simulation Result.

Figure 5 is a plot detailing the coverage of the satellite constellation by overlaying the XYZ Earth-rotation adjusted coordinates over a sphere representing Earth. The observatories are also on this plot, but they are not visible due to the density of points.

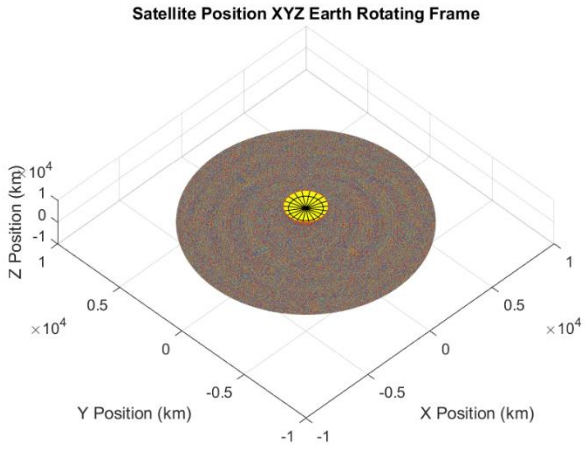

Figure 5. LEO Orbit Coverage Simulation Result.

The plot shown in Figure 6 is a detailed ground track. The black dots are the observatories. The satellite ground track points are so dense they appear as one block of color.

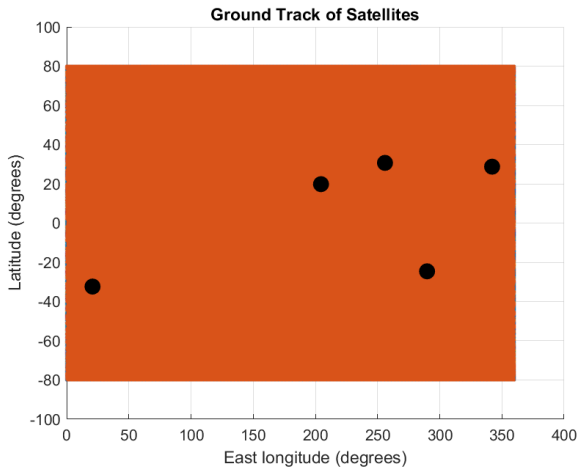

Figure 6. LEO Orbit Ground Track Simulation Result.

The set of images in Figures 7 through 11 shows the satellites that intersect each observatory and the data reduction associated with the analysis. The leftmost plot shows all the intersections, the middle plot includes the satellites that are illuminated, and the last plot shows the satellites that are illuminated while the observatory is in darkness. The red points are the intersections within 1 degree FOV, the blue points are the intersections within 5 degrees, and the green points are the intersections within 10 degrees.

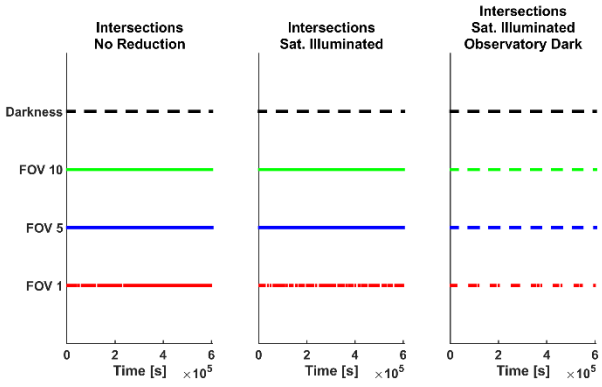

Figure 7. LEO Observatory 1 Intersections.

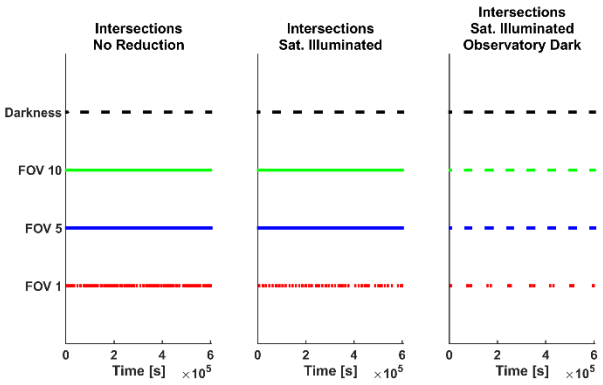

Figure 8. LEO Observatory 2 Intersections.

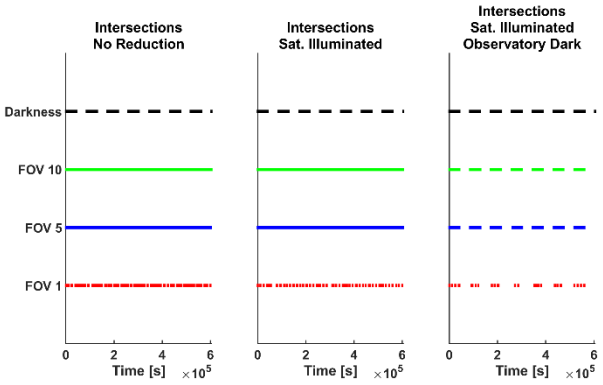

Figure 9. LEO Observatory 3 Intersections.

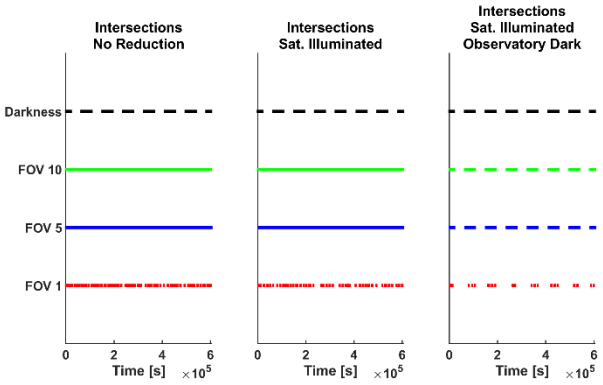

Figure 10. LEO Observatory 4 Intersections.

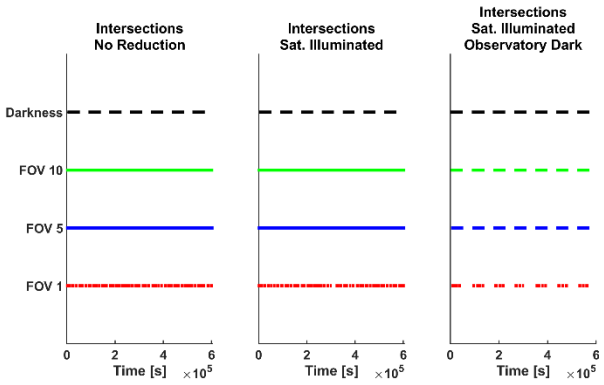

Figure 11. LEO Observatory 5 Intersections.

MEO Results

Figure 12 shows the set of satellite orbits from an Earth-fixed nonrotating frame. This plot is a check to ensure that the orbits are correctly matching what the CBO theoretical constellation specified.

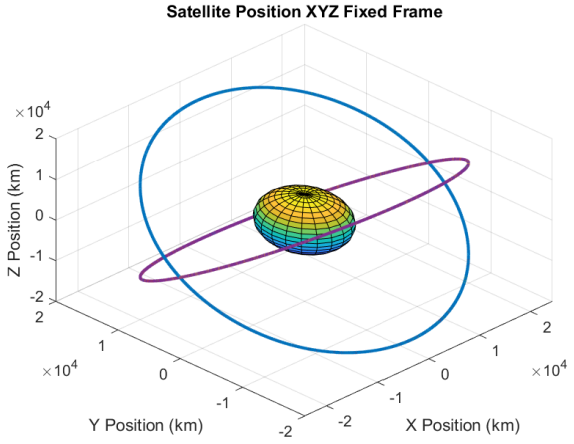

Figure 12. MEO Orbit Track Simulation Result.

Figure 13 is a plot detailing the coverage of the satellite constellation by overlaying the XYZ Earth-rotation adjusted coordinates over a sphere representing Earth. The observatories are also on this plot and are visible unlike with the LEO plot.

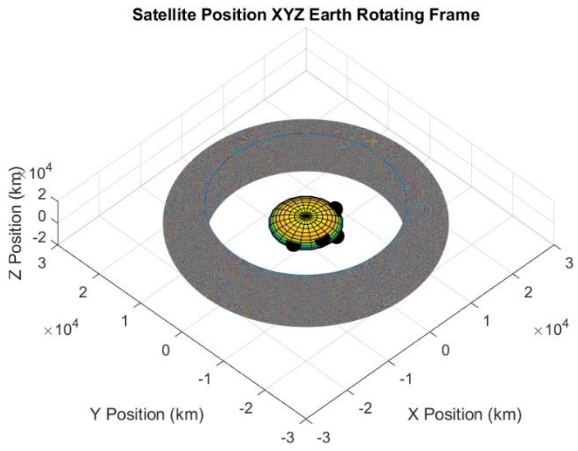

Figure 13. MEO Orbit Coverage Simulation Result.

Figure 14 is a detailed ground track. The black dots are the observatories. The satellite ground track points are so dense they appear as one block of color.

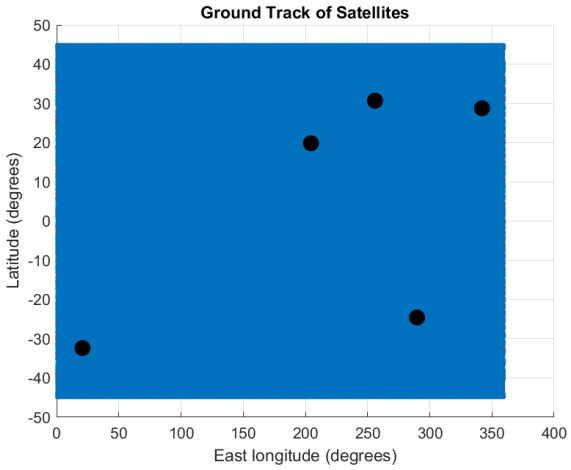

Figure 14. MEO Orbit Ground Track Simulation Result.

The set of images in Figures 15 through 19 shows the satellites that pass through each observatory and the data reduction associated with the analysis. The leftmost plot shows all the intersections, the middle plot includes the satellites that are illuminated, and the last plot shows the satellites that are illuminated while the observatory is in darkness. The red points are the intersections within 1 degree FOV, the blue points are the intersections within 5 degrees, and the green points are the intersections within 10 degrees. Unlike with the LEO plots, the MEO plots do not show a reduction in intersections based on illumination.

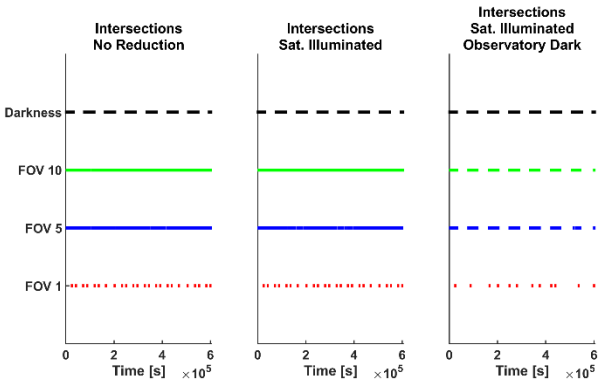

Figure 15. MEO Observatory 1 Intersections.

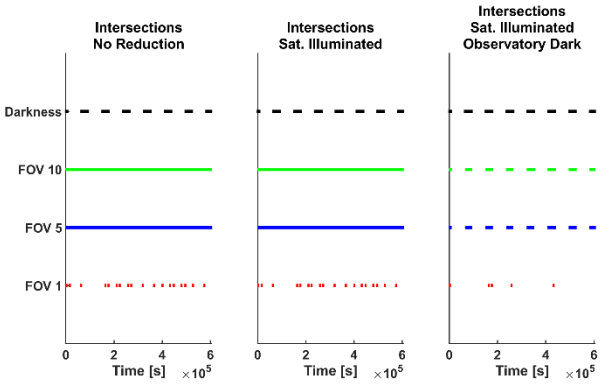

Figure 16. MEO Observatory 2 Intersections.

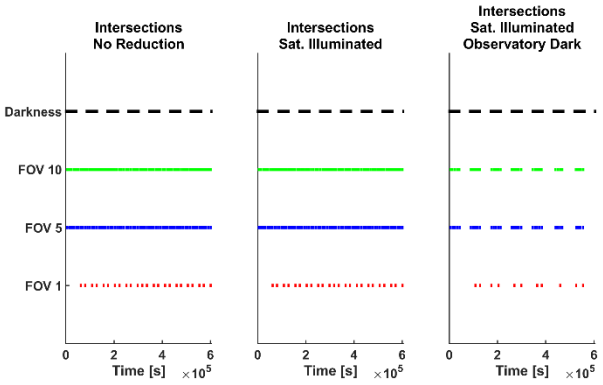

Figure 17. MEO Observatory 3 Intersections.

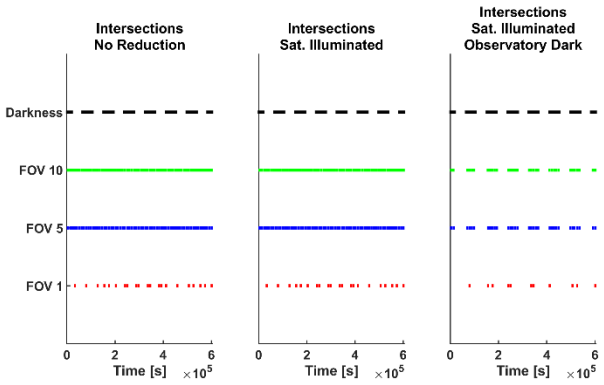

Figure 18. MEO Observatory 4 Intersections.

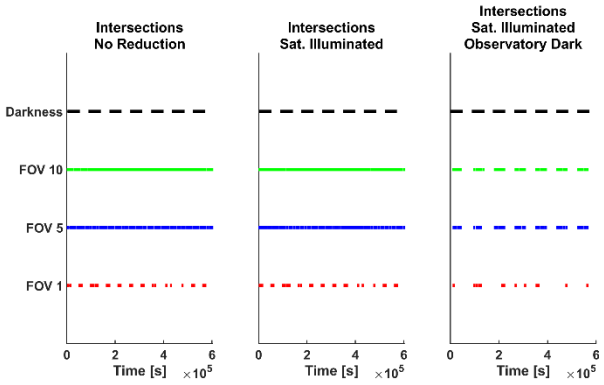

Figure 19. MEO Observatory 5 Intersections.

Tabulated Results

The tabulated results, shown in Tables 2 and 3, are derived from the plots above. The percentage value is calculated by counting all of the intersected points, with all of the points in darkness for each observatory. The percentage is denoted as % FOV X, and the count is denoted as # FOV X. The hours lost, FOV X Hrs Lost, is computed by multiplying the number of intersected points by the delta time, then converting the result into hours. These hours lost are over a 7-day period of nights, which is 84 hours.

Table 2. LEO Results Table.

	FOV 1			FOV 5			FOV 10		
Loc.	**%**	**#**	**Hrs Lost**	**%**	**#**	**Hrs Lost**	**%**	**#**	**Hrs Lost**
1	0.079	48.000	0.067	1.763	1066.000	1.481	5.517	3337.000	4.635
2	0.067	27.000	0.038	1.319	532.000	0.739	4.052	1634.000	2.269
3	0.056	34.000	0.047	1.442	872.000	1.211	4.697	2841.000	3.946
4	0.051	31.000	0.043	1.539	931.000	1.293	5.058	3059.000	4.249
5	0.076	46.000	0.064	1.913	1157.000	1.607	5.969	3610.000	5.014

Note: Loc. = location.

Table 3. MEO Results Table.

	FOV 1			FOV 5			FOV 10		
Loc.	**%**	**#**	**Hrs Lost**	**%**	**#**	**Hrs Lost**	**%**	**#**	**Hrs Lost**
1	0.020	12.000	0.017	0.410	248.000	0.344	1.316	796.000	1.106
2	0.012	5.000	0.007	0.387	156.000	0.217	1.203	485.000	0.674
3	0.018	11.000	0.015	0.466	282.000	0.392	1.445	874.000	1.214
4	0.018	11.000	0.015	0.479	290.000	0.403	1.516	917.000	1.274
5	0.021	13.000	0.018	0.511	309.000	0.429	1.619	979.000	1.360

CONCLUSION

Clearly, both LEO and MEO constellations impact observatories through the loss in usable hours. Because the LEO constellation has more satellites than the MEO constellation, it had three to five times more intersections on average than the MEO constellation and approximately the same factor in observatory time lost due to intersections.

The illumination of the satellites did not affect MEO satellites as they have significantly more altitude than the LEO satellites, which were affected as they spend more time in Earth's shadow.

However, the plots show that the duration of the satellite passes affects the usable observatory time. This effect is more pronounced with LEO satellites than with MEO satellites as LEO satellites are more frequently over the observing sites, even though they travel faster than the MEO satellites.

The impact to the observatories in Table 1 will hinder astronomy as the deep FOV observatories are critical to new discoveries. They are the most sensitive due to wide FOVs and large apertures, which let in more light. However, when taking into account only one LEO and one MEO constellation, the effects for the observatories over the 84 hours of darkness are small, with the maximum number of hours lost at around 5 hours and the minimum mere minutes. This result is highly conservative as there are multiple existing LEO and MEO constellations with more being launched. A simulation that includes all existing LEO and MEO constellations would show a further decrease in the usable observatory hours.

A further impact of LEO and MEO constellations on observatories is a reduction in the ability to conduct long exposures. The spacing of hours lost (shown on Figures 7 through 11 and Figures 15 through 19) indicates that the frequent passes of satellites have shrunk long observing windows.

REFERENCES

[1] Government Accountability Office. “Large Constellations of Satellites: Mitigating Environmental and Other Effects.” (GAO Publication No. 22-105166). Washington, D.C.: U.S. Government Printing Office, 2022.

[2] Congressional Budget Office. “Large Constellations of Low-Altitude Satellites: A Primer.” (CBO Publication No. 58794). Washington, D.C.: U.S. Government Printing Office, 2023.

[3] O.R. Hainaut and A.P. Williams, “Impact of Satellite Constellations on Astronomical Observations with ESO Telescopes in the Visible and Infrared Domains.” *Astronomy & Astrophysics*. Vol. 636, A121, April 2020.

[4] C. Walker, “Impact of Satellite Constellations on Optical Astronomy and Recommendations Toward Mitigations,” *Bulletin of the American Astronomical Society*, Vol. 52, No. 2, 0206, August 2020.

[5] H.D. Curtis, *Orbital Mechanics for Engineering Students*. Butterworth-Heinemann, Amsterdam, 2021.

[6] P.R. Escobal, *Methods of Orbit Determination*. Robert E. Krieger Pub, Malabar, Florida, 1976.